Geography and Sustainability 2 (2021) 163–174

Contents lists available at ScienceDirect

Geography and Sustainability

journal homepage: www.elsevier.com/locate/geosus

Overview of recent land cover changes, forest harvest areas, and soil erosion trends in Nordic countries[1]

Na Zhou[1,2,#], Xiangping Hu[2,#,*], Ingvild Byskov[2], Jan Sandstad Næss[2], Qiaosheng Wu[1,**], Wenwu Zhao[3], Francesco Cherubini[2]

[1] School of Economics and Management, China University of Geosciences, Wuhan 430074, China
[2] Industrial Ecology Program, Department of Energy and Process Engineering, Norwegian University of Science and Technology, N-7491, Trondheim, Norway
[3] State Key Laboratory of Earth Surface Processes and Resource Ecology, Faculty of Geographical Science, Beijing Normal University, Beijing 100875, China

HIGHLIGHTS

- We investigate recent 27-year land cover dynamics in four Nordic countries.
- Wetland showed the strongest reduction, followed by forest and sparse vegetation.
- Forest harvest areas have a non-negligible overlap with forest transition.
- Soil erosion rates in Nordic are low but with exacerbating locations in Norway.

GRAPHICAL ABSTRACT

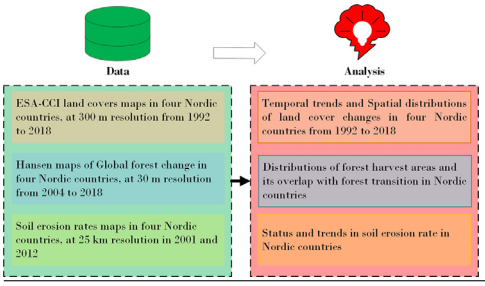

ARTICLE INFO

Article history:
Received 16 November 2020
Received in revised form 20 July 2021
Accepted 22 July 2021
Available online 28 July 2021

Keywords:
Land cover changes
Spatiotemporal analysis
Forest management
Soil erosion

ABSTRACT

Mapping spatiotemporal land cover changes offers opportunities to better understand trends and drivers of environmental change and helps to identify more sustainable land management strategies. This study investigates the spatiotemporal patterns of changes in land covers, forest harvest areas and soil erosion rates in Nordic countries, namely Norway, Sweden, Finland, and Denmark. This region is highly sensitive to environmental changes, as it is experiencing high levels of human pressure and among the highest rates of global warming. An analysis that uses consistent land cover dataset to quantify and compares the recent spatiotemporal changes in land cover in the Nordic countries is missing. The recent products issued by the European Space Agency and the Copernicus Climate Change Service framework provide the possibility to investigate the historical land cover changes from 1992 to 2018 at 300 m resolution. These maps are then integrated with time series of forest harvest areas between 2004 and 2018 to study if and how forest management is represented in land cover products, and with soil erosion data to explore status and recent trends in agricultural land. Land cover changes typically involved from 4% to 9% of the total area in each country. Wetland showed the strongest reduction (11,003 km^2, −11% of the wetland area in 1992), followed by forest (8,607 km^2, −1%) and sparse vegetation (5,695 km^2, −7%), while agriculture (15,884 km^2, 16%) and settlement (3,582 km^2, 84%) showed net increases. Wetland shrinkage dominated land cover changes in Norway (5,870 km^2, −18%), followed by forest and grassland with a net gain of 3,441 km^2 (3%) and 3, 435 km^2 (10%), respectively. In Sweden, forest areas decreased 13,008 km^2 (−4%), mainly due to agriculture expansion (9,211 km^2, 29%). In Finland, agricultural areas increased by 5,982 km^2 (24%), and wetland decreased by 6,698 km^2 (−22%). Settlement had the largest net growth in Denmark (717

[1] Given his role as Associate Editor of this journal, Wenwu Zhao had no involvement in the peer-review of this article and has no access to information regarding its peer-review. Full responsibility for the peer-review process for this article was delegated to Carla Sofia Santos Ferreira.

* Corresponding author: Xiangping Hu
E-mail addresses: Xiangping.Hu@ntnu.no (X. Hu), qshwu@cug.edu.cn (Q. Wu).
# These authors contributed equally
** Co-Corresponding author: Qiaosheng Wu

https://doi.org/10.1016/j.geosus.2021.07.001

km^2, 70%), mainly from conversion of agriculture land. Soil erosion rates in Nordic countries are lower than the global average, but they are exacerbating in several locations (especially western Norway). The integration of the land cover datasets with maps of forest harvest areas shows that the majority of the losses in forest cover due to forestry operations are largely undetected, but a non-negligible share of the forest-to-agriculture (up to 19%) or forest-to-grassland (up to 51%) transitions overlap with the harvested sites. Forestry activity in the study region primarily involves small-scale harvest events that are difficult to be detected at the 300 m resolution of the land cover dataset. An accurate representation of forest management remains a challenge for global datasets of land cover time series, and more interdisciplinary international efforts are needed to address this gap. Overall, this analysis provides a detailed overview of recent changes in land cover and forest management in Nordic countries as represented by state-of-the-art global datasets, and offers insights to future studies aiming to improve these data or apply them in land surface models, climate models, landscape ecology, or other applications.

1. Introduction

Influenced by anthropogenic drivers and climate warming, changes in land cover are an important indicator of global environmental change (Henriksen and Hilmo, 2015; Saco et al., 2018; Song et al., 2018; Huang et al., 2020; Hu et al., 2021b), and play a key role for climate change mitigation, sustainable food supply, and nature conservation (Mousivand and Arsanjani, 2019; Roe et al., 2019; Smith et al., 2020). Historically, land cover changes primarily occurred as deforestation due to agriculture expansion and urbanization (Arsanjani et al., 2013; Nunes et al., 2016; Leirpoll et al., 2021). Land covers reflect the distribution characteristics of surface vegetation and ecosystems (Szogs et al., 2017), and monitoring their spatial differentiation and evolution trend is instrumental in more sustainable plans of regional ecological environments, reducing carbon emissions, and preventing biodiversity losses and soil erosion (Crooks et al., 2017; Cherubini et al., 2018b; Pei et al., 2018; Taubert et al., 2018; Ren et al., 2020; Hu et al., 2021a). A detailed understanding of land use dynamics is also crucial for successful implementation of various programs within climate change mitigation (Cherubini et al., 2018a; Hu et al., 2019; Duveiller et al., 2020; Huang et al., 2020), food security (Gomes et al., 2019; Gava et al., 2020), renewable energy supply (Leirpoll et al., 2021; Næss et al., 2021), and nature conservation (Leclère et al., 2020; Strassburg et al., 2020).

Based on satellite remote sensing data, many global and regional land cover datasets have been produced, resulting in a variety of global and regional land cover products (Grekousis et al., 2015), with different land cover classifications, accuracy, resolution and time periods (Mousivand and Arsanjani, 2019). One of the first global land cover products is the International Geosphere-Biosphere Program's Data and Information System (Loveland and Belward, 1997), developed by the U.S. Geological Survey and the European Commission's Joint Research Centre, containing 17 classes with 1 km spatial resolution. The European Commission issued another global land cover product GLC2000 with 1 km resolution and 22 classes (Bartholome and Belward, 2005). The GlobeLand30 dataset released in China contains 10 landcover types with 30 m resolution (Chen et al., 2015). Global land cover mapping from Moderate Resolution Imaging Spectroradiometer (MODIS) combines five land cover classification schemes at an annual time step from 2001 at 1 km resolution (Friedl et al., 2002). The Land-use Harmonization 2 project aims to smoothly connect updated historical reconstructions of land-use with new future projections, and recently produced a dataset at a resolution of 0.25 × 0.25 degree over a long time period (850–2100, with extensions to 2300) (Hurtt et al., 2020). All these datasets only cover specific years or individual years, or, when time-series are available, they have relatively coarse resolutions. The recently released ESA climate change initiative land cover products (ESA-CCI-LC) provide time series of global land cover maps for 37 land cover categories from 1992 to 2015 at a high spatial resolution of 300 m at the equator (ESA, 2017). This was followed by consistent maps from Copernicus Climate Change Service climate data store and land cover products (C3S-CDS-LC) from 2016 to 2018 (C3S, 2019). The method used and characteristics of the 2016 to 2018 land cover maps are consistent with the process used to create the ESA-CCI-LC maps. These datasets combine multiple remote sensing products and ground-truth observations, and they were specifically developed to advance a more realistic representation of land cover dynamics in climate models (Plummer et al., 2017). The ESA-CCI-LC dataset was also used to characterize temporal dynamics and spatial patterns of changes in land cover at a landscape and global level (Liu et al., 2018a; Liu et al., 2018b; Mousivand and Arsanjani, 2019). Existing studies used the ESA-CCI-LC dataset to investigate aggregated global land cover changes (Liu et al., 2018a; Mousivand and Arsanjani, 2019; Hu et al., 2021b). For example, Mousivand and Arsanjani (2019) analyzed the gains and losses of different land cover types around the world from the year 1992 to 2015 and predicted the changes of different land cover types in 2030 and 2050. They, however, did not point out the specific locations of the changes. Hu et al. (2021b) recently analyzed the land cover dynamics using ESA-CCI-LC and C3S-CDS-LC products, but the analysis focused on the global scale with no country specific insights.

There is an underrepresentation of boreal and arctic regions in the available European land use and land cover literature (Plieninger et al., 2016). To the best of our knowledge, an analysis that uses consistent dataset to quantify and compare the recent spatiotemporal changes in land cover in the Nordic countries is missing. This region is highly sensitive to environmental changes as it is experiencing high human pressure (agriculture, forestry, and urban expansion) and the highest rates of global warming (IPCC, 2019). Existing research mainly focused on specific changes and effects, such as forest characteristics and key climatic variables (Lukes et al., 2016; Cherubini et al., 2017; Iordan et al., 2018a), biodiversity loss (Auffret et al., 2018; Iordan et al., 2018b; Fourcade et al., 2019), grassland restoration (Milberg et al., 2019), water risk (Räsänen et al., 2018), carbon reserves (Vauhkonen and Packalen, 2018) and wood outtake potentials (Hu et al., 2018). The Nordic region is highly developed, but population densities, land use characteristics, and the corresponding human footprint vary across the region (Venter et al., 2016). For example, cropland is the most extensive land use in Denmark (Karvonen et al., 2018; Osei-Owusu et al., 2019; Vogdrup-Schmidt et al., 2019) but it is much less present in other Nordic countries (Strand, 2013; (FAO, 2020)). Forests cover large parts of Norway, Sweden and Finland (FAO, 2020), with the majority being managed forests periodically exposed to harvest (Ceccherini et al., 2020). It is largely unclear how forest harvest areas are detected by the ESA-CCI-LC and C3S-CDS-LC products, and there are risks that they are reported as transitions of forest to other types of land cover (e.g., agriculture or grassland). The intensive management of forests in Nordic countries make them the ideal case for studying this issue. There are also dynamics other than management that are influencing changes in forest areas in Nordic countries. Anthropogenic activities such as domestic grazing have historically kept the forest extent down in outfield areas, but recently reduced grazing intensity has spurred natural forest regrowth (Wehn et al., 2012; Mienna et al., 2020). Owing to the polar amplification effect, the Nordic region is experiencing the highest rates of global warming in the world, affecting land use dynamics such as tree lines (Bryn and Potthoff, 2018), greening of bare area and scarce vegetated areas (Myers-Smith et al., 2020), and higher risks of wetland drying

(Lohila et al., 2010; Werner et al., 2013). Forest clearance has also occurred due to recent urban expansion (van Vliet, 2019). Agricultural intensification has led to increased homogenization of Nordic landscapes, with both cropland expansion into previously mosaic landscapes, and forest expansion into newly abandoned marginal areas (Auffret et al., 2018; Aune et al., 2018). Agricultural landscapes in Nordic countries also face challenges of soil erosion, and more research is needed to better understand the interplay between human driving forces and the climatic drivers (wind and precipitation), in order to take measures against erosion (Ulén et al., 2012).

The purpose of this study is to investigate the recent land cover changes and land transitions from 1992 to 2018 in Norway, Sweden, Finland, and Denmark, as represented by the ESA-CCI-LC and C3S-CDS-LC datasets. Hereafter the name CCI-LC dataset is used when these two land cover datasets are combined. This analysis shows where land covers are distributed and where the major transitions occurred, as well as the changes in soil erosion associated with agriculture activities. We also identify areas of forest harvest from another independent dataset and investigate the overlap between clear-cut areas and forest transitions to other land covers (agriculture, grassland, sparse vegetation, and shrubland) in order to investigate how forest management is represented by the CCI-LC dataset.

2. Methodology

2.1. Land cover datasets

The original land cover data is from the land cover maps issued by ESA and the European Centre for Medium-Range Weather Forecasts. The maps have a spatial resolution of 0.002,778 degree (approximately 300 m at the equator) on an annual basis from 1992 to 2018. The data until 2015 come from the ESA-CCI-LC product (V2.0.7b), and from 2016 to 2018 from the C3S-CDS-LC product (V2.1.1). The two products are highly consistent and use the classification system developed by the United Nations Food and Agriculture Organization, which divides the global land cover into 37 classes. To more accurately map and quantify changes in land cover at the regional and national levels, the more generic IPCC land classification is used to regroup the original 37 land cover classes into 9 classes using a cross-walking table (Table 1). Thanks to this, we can avoid false detection between semantically close land cover classes (ESA, 2017).

2.2. Trends of land cover changes

For each Nordic country, we calculated the interannual changes in land cover class relative to 1992 using Equation (1).

$$\text{Area Change}_{i,\,j,\,t} = \frac{\text{Area}_{i,\,j,\,t}}{\text{Area}_{i,\,j,\,1992}} \tag{1}$$

where *i, j, t* is the index for land cover classes, countries, and year, respectively. $\text{Area}_{i,j,t}$ denotes the area of land cover type i in country j in year t. Due to the curvature of the earth, areas of grids with 300 m resolution at the equator are varying with latitude and can be obtained by Equation (2).

$$A_q = \frac{\pi r^2 \times \left|\text{lon}_2 - \text{lon}_1\right| \times \left|\sin\left(\text{lat}_2\right) - \sin\left(\text{lat}_1\right)\right|}{180} \tag{2}$$

where, A_q is the calibrated area of grid q, lon_1, lon_2, lat_1 and lat_2 are the longitude and latitude of the grid q, r is the earth radius. For a given year t, the total area of land cover type i in country j is calculated by Equation (3),

$$\text{Area}_{i,\,j,t} = \sum_{q=1}^{N} A_q \tag{3}$$

where N denotes the total number of grids of land cover type i in country j at 300 m resolution. The analysis of land cover changes is based on the original spatial resolution (300 m) of the CCI-LC dataset, and lower resolutions are only used in the figures of the results for visualization purposes.

2.3. Land cover transition analysis

To explore the typical characteristics of changes in land cover in the four Nordic countries, we quantified the land cover transitions for each pair of land cover classes between 1992 and 2018 by a transition matrix. In the transition matrix, each element is the area that changed from one category to another. For instance, the element in the p-th row and q-th column of the transition matrix is the area of land cover transition from land cover class p in 1992 to land cover class q in 2018, and the area of transition was obtained by summing all the pixels areas obtained from Equation (2) for all the grids that are classified as land cover class p in 1992 but as land cover class q in 2018 when $p \neq q$. When $p = q$, the element in the transition matrix is set to 0.

We also investigate the spatial patterns of changes in land cover. We first identify the land cover gains (coded as +1) and losses (coded as −1) in each pixel with the original 300 m resolution for each land cover class. If there is no change in the pixel, it is coded as 0. We then aggregate the results to 9 km resolution and calculate the area ratio of the changes in the aggregated grid. This aggregation helps to better visualize the spatial distribution of the changes in each land cover.

2.4. Forest management in Nordic countries

In the four studied Nordic countries, forests have been under intensive management (Schelhaas et al., 2018; Ceccherini et al., 2020), and practices of sustainable forest management have been pursuing to achieve ecosystem services such as carbon sequestration, wood production, nature conservation and climate change mitigation. Common harvest methods focus on limited area extents, with forest patches kept under rotation, and in Finland and Sweden thinning is more common than in Norway. About 50% of the forest clear-cut areas in Finland involve patches larger than 7 ha, and about 20% of the harvested sites are between 3.5 and 7 ha (the rest occurs in areas smaller than 3.5 ha) (Ceccherini et al., 2020). In Sweden, the average size of clear-cut areas larger than 7 ha is about 75%, whereas in Denmark it is much smaller (20%).

It is largely unclear if and how forest harvest areas are detected by the CCI-LC product. Given the average smaller extent of harvested areas than the resolution of the land cover maps, they might be undetected or reported as forest transition, most likely agriculture, grassland, sparse vegetation or shrubland. We investigate the potential overlap between forest transitions and forest harvest area using the global forest change (GFC) maps from Hansen et al. (2013). These GFC maps provides yearly estimates of tree cover change (gains and losses) relative to 2000 with a spatial resolution of approximately 30 m (at the equator), and they are available in Google Earth Engine (GEE) (Gorelick et al., 2017). GEE is a platform containing a huge amount of Earth Science data and provides parallel cloud-computing and geospatial operation with lots of ready-to-use functions. Ceccherini et al. (2020) used the GEE platform to investigate the harvested (clear-cut only) forest areas over 26 European countries by detecting the forest cover changes which were attributed to either forest management, i.e., forest harvest, or disturbance due to fire and windstorms. They assumed that windstorms cause larger area losses than forest management, and they thus filtered out the losses that are three times the median absolute deviation away from the median. The European forest fire information system dataset is used to mask out burned forest (EFFIS, 2019). The remaining losses in forest cover can thus be treated as a proxy for forest harvest area.

We aggregate the GFC forest loss maps to 300 m, i.e., the same spatial resolution of our land cover datasets, and compute the annual percentage of forest losses between 2004 and 2018 using the GEE platform. We then post process the results to obtain the forest harvest maps following

Table 1
Conversion of the original land cover classes in CCI-LC dataset into the standard IPCC land cover classes (based on ESA (2017) cross-walking table). AGR: agriculture, FOR: forest, GRA: grassland, WET: wetland, SET: settlement, SHR: shrubland, SPA: sparse vegetation, BAR: bare area, WAT: water, SNO: permanent snow and ice.

IPCC classes		Code	Legend used in the CCI-LC product
1	AGR	10, 11, 12	Rainfed cropland
		20	Irrigated cropland
		30	Mosaic cropland (> 50%) / natural vegetation (tree, shrub, herbaceous cover) (< 50%)
		40	Mosaic natural vegetation (tree, shrub, herbaceous cover) (> 50%) / cropland (< 50%)
2	FOR	50	Tree cover, broadleaved, evergreen, closed to open (> 15%)
		60, 61, 62	Tree cover, broadleaved, deciduous, closed to open (> 15%)
		70, 71, 72	Tree cover, needleleaved, evergreen, closed to open (> 15%)
		80, 81, 82	Tree cover, needleleaved, deciduous, closed to open (> 15%)
		90	Tree cover, mixed leaf type (broadleaved and needleleaved)
		100	Mosaic tree and shrub (> 50%) / herbaceous cover (< 50%)
		160	Tree cover, flooded, fresh or brackish water
		170	Tree cover, flooded, saline water
3	GRA	110	Mosaic herbaceous cover (> 50%) / tree and shrub (< 50%)
		130	Grassland
4	WET	180	Shrub or herbaceous cover, flooded, fresh-saline or brackish water
5	SET	190	Urban
6	SHR	120, 121, 122	Shrubland
7	SPA	140	Lichens and mosses
		150, 151, 152, 153	Sparse vegetation (tree, shrub, herbaceous cover)
8	BAR	200, 201, 202	Bare areas
9	WAT	210	Water

the approach described by Ceccherini et al. (2020). These forest harvest maps are integrated with the land cover maps to investigate the extent to which forest harvest areas overlap with the forest transition reported by the CCI-LC products using the following Equation (4):

$$r_j = \frac{\text{area}_{j,\ \text{forest harvest}} \cap \text{area}_{j,\ \text{for}\rightarrow\text{agr}}}{\text{area}_{j,\ \text{for}\rightarrow\text{agr}}} \tag{4}$$

where r_j is the overlap ratio, $\text{area}_{\text{forest harvest}}$ is the area of harvested forest, $\text{area}_{\text{for}\rightarrow\text{agr}}$ is the area of forest to agriculture transition, j is the index of country, and $\cap$ is the logical conjunction operator. The same procedure is used for the other types of possible transitions that can represent forest management: forest to grassland, forest to sparse vegetation and forest to shrubland. We further investigate the trends of the forest harvest in the four Nordic countries. The areas of annual forest harvest from 2004 to 2018 in Sweden, Denmark and Finland can be directly obtained from Ceccherini et al. (2020) while the annual forest harvest areas in Norway are estimated following the same approach given by Ceccherini et al. (2020).

2.5. Changes of soil erosion

We explore the changes in soil erosion rates (SERs) due to agriculture activity in Nordic countries using the SER maps from Borrelli et al. (2017), which contains the information on SER for 2001 and 2012. The SER maps are obtained using a model approach based on the revised universal soil loss equation (RUSLE) (De Vente and Poesen, 2005). The RUSLE-based modelling approach is widely used for predicting soil erosion (Borrelli et al., 2017; Borrelli et al., 2020) and provides estimates of potential soil displacement rates by water erosion (De Vente and Poesen, 2005). The SER maps provided by Borrelli et al. (2017) further considered the land cover types, their dynamics and farming system. Following Hu et al. (2021b), we assume that SER changed linearly during the two years,

$$k_{q,j} = \frac{\text{SER}_{q,j,2012} - \text{SER}_{q,j,2001}}{\Delta t} \tag{5}$$

for grid q in country j, and $\Delta t = 11$. In Equation (5), only the grid q that is classified as agriculture both in 2001 and 2012 was considered to single out soil erosion due to agriculture activity. With Equation (5), the total increased soil erosion in country j (denoted as ΔSE_j) in the period 2001-2012 was obtained as follows

$$\Delta\text{SE}_j = \sum_q \int_0^{11} k_{q,j}\, t\, dt \times A_q = \frac{11}{2} \sum_q \left(\text{SER}_{q,j,2012} - \text{SER}_{q,j,2001}\right) \times A_q \tag{6}$$

where $k_{q,j}$ is given in Equation (5), and A_q is the area of grid q. In Equation (6), the sum is only over grid q that is classified as agriculture both in 2001 and in 2012.

3. Results

3.1. Variation of land covers

Table 2 shows the area of each land cover in the four Nordic countries in 1992 and 2018 according to the dataset processed in this analysis. Forest is by far the largest type of surface cover in Norway, Sweden and Finland, accounting for more than 40% of the total area in each country. Agricultural land is the most common land cover type in Denmark. Despite having the smallest population, Norway has the largest extent in urban settlements in Nordic countries. A similar extent of wetland areas is present in all the Nordic countries, while grassland and sparse vegetation are mainly abundant in Norway and Sweden.

The trends in land cover changes are compared in terms of normalized interannual changes between 1992 and 2018 in Fig. 1. Agriculture remained relatively constant (or slightly reduced) in Denmark, but it almost linearly increased in the other three countries (at a higher pace in Sweden and Finland than Norway). Relative changes in forest areas were smaller than those in other land covers, largely due to the abundant forest areas in the countries that minimize the normalized changes in this land use type. Forest areas increased in all countries at a similar rate, except for Sweden, where forest areas steadily declined. Both grassland and bare area in Finland show high normalized gains, while variations are limited in the other countries. This might be due to the limited area extent of these two land cover types in Finland, which make normalized results very sensitive to even small changes in areas. Wetland is firmly declining in Norway and Finland, while settlement expands in every country (especially in Norway). Shrubland and sparse vegetation show contrasting trends, especially in Finland. These land cover classes are very similar in terms of vegetation cover, and their distinction in the land cover dataset is challenging. Their univocal identification and interchanges should be interpretated with care. More explanations about the drivers of these changes are provided in the following sections.

Table 2
Area of each land cover in the four Nordic countries in 1992 and 2018 (Unit: 1,000 km^2). AGR: agriculture, FOR: forest, GRA: grassland, WET: wetland, SET: settlement, SHR: shrubland, SPA: sparse vegetation, BAR: bare area, WAT: water.

	Norway		Sweden		Finland		Denmark	
Categories	1992	2018	1992	2018	1992	2018	1992	2018
AGR	13.48	15.13	32.02	41.23	24.48	30.47	32.29	31.33
FOR	137.60	141.04	309.79	296.79	238.58	239.42	5.26	5.38
GRA	35.77	39.20	17.41	19.01	1.16	1.94	2.84	2.99
WET	31.88	26.01	32.40	33.96	31.13	24.43	0.66	0.66
SET	1.69	3.54	1.13	1.98	0.44	0.60	1.03	1.75
SHR	3.19	3.19	0.38	0.63	0.23	0.39	0.00	0.00
SPA	61.97	58.93	14.43	13.82	6.66	4.62	0.01	0.01
BAR	17.61	17.44	2.68	2.74	0.18	0.38	0.06	0.06
WAT	29.58	28.28	43.22	43.30	36.26	36.89	3.51	3.48

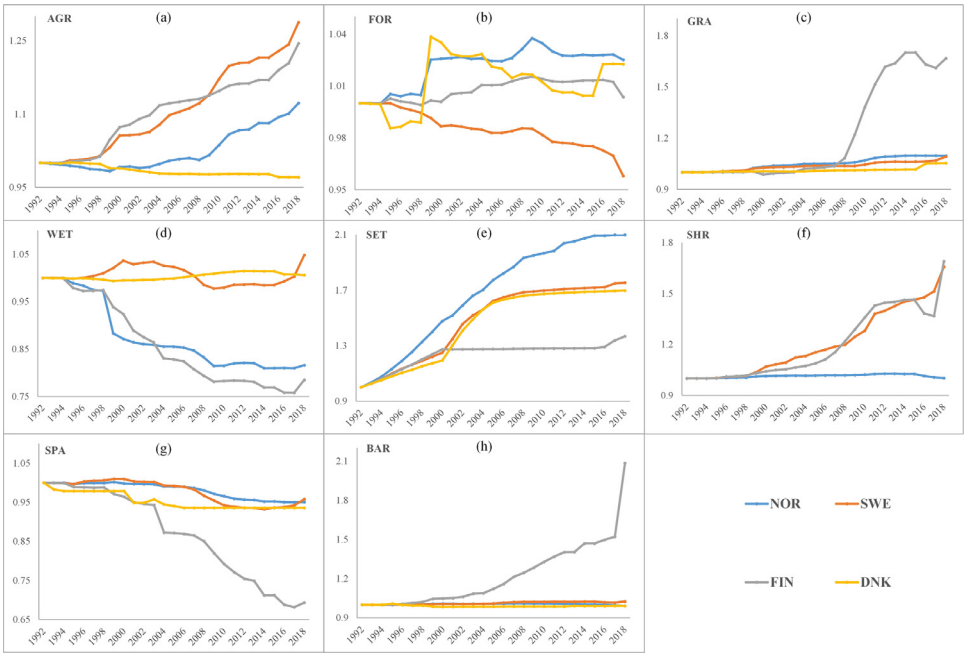

Fig. 1. Area changes of each land cover class relative to its extent in 1992 for each Nordic country. Lines of different colors with solid dots represent the four Nordic countries: blue for Norway (NOR), orange for Sweden (SWE), grey for Finland (FIN) and yellow for Denmark (DNK). The horizontal axis is the study period, and the vertical axis is the area change of each year relative to 1992. Values higher than 1 show an increase relative to 1992, while values smaller than 1 indicate a decrease. AGR: agriculture, FOR: forest, GRA: grassland, WET: wetland, SET: settlement, SHR: shrubland, SPA: sparse vegetation, BAR: bare area.

In general, the interpretation of these trends should consider that they refer to the changes relative to the area extension within each country in 1992, and they are highly sensitive to the initial extent of the particular type of land cover in a given country. For example, large normalized changes in one land cover in one country can correspond to much smaller hectares of land than a country that showed minimal increases in normalized values, if the latter country had a much larger presence of the land cover in question in 1992. Results in Fig. 1 are thus to be interpreted together with the absolute values in Table 2.

3.2. Land cover transitions in Nordic countries

The net trends of land cover transitions in the four countries from 1992 to 2018 are shown in Fig. 2. In Norway, the dominant net change in land cover is a net loss of 5,870 km^2 in wetland, which is about 18% of the wetland area in 1992. Wetland mostly transitioned to forest, because of progressive wetland drying due to climate change, water drainage and other anthropogenic factors such as excessive water withdrawals or eutrophication (Lohila et al., 2010; Werner et al., 2013). Agriculture, forest, and grassland show a net gain of 1,650 km^2 (12%), 3,441 km^2 (3%) and 3,435 km^2 (10%), respectively (Fig. 2a). The gross area gain of settlement is 1,857 km^2, of which 59% and 31% are derived from forest and agriculture, respectively. In Norway, 46% of the reductions in sparse vegetation is due to conversion to grassland, and 42% is converted to forest. The latter is also observed in Finland, and can be associated to reduced human pressure, e.g., decreasing grazing rates (Mienna et al., 2020), and/or accelerated vegetation growth caused by climate change (Kellomäki et al., 2018). In Sweden, there is a net loss in forest area of 13,008 km^2 (−4%), mainly caused by an expansion of agriculture, making it the largest net gain (9,211 km^2, 29%) (Fig. 2b). The primary sources of settlement expansion are agriculture and forest, which accounted for 45% and 43% of Sweden's settlement gross gain, respectively. Forest shows the largest gross increase in Finland, and wetland was its largest source, making wetland the largest net loss (6,698 km^2, −22%). In contrast, agriculture was the country's largest net gain (5,982 km^2) which increased by 24% compared to 1992, mainly from forest (Fig. 2c). The absolute net area changes of settlement, shrubland, and bare area in Finland were relatively small compared with other land covers, which were 160 km^2, 160 km^2, and 198 km^2, respectively. Due to the low proportion of the above three land covers in Finland, however, the relative changes of these land cover classes were 37%, 69%, and 108% respectively. The area taken from forest was the leading source of Finland's settlement expansion, accounting for 67% of the gross gain (180 km^2), and the contribution of agriculture was 21% (34 km^2). During the study period, settlement has the largest net growth in Denmark (717 km^2, 70%), mainly transitioned from agriculture land (Fig. 2d). Besides, the area of forest and grassland also showed a net increase, while agriculture showed the largest net reduction (956 km^2, −3%).

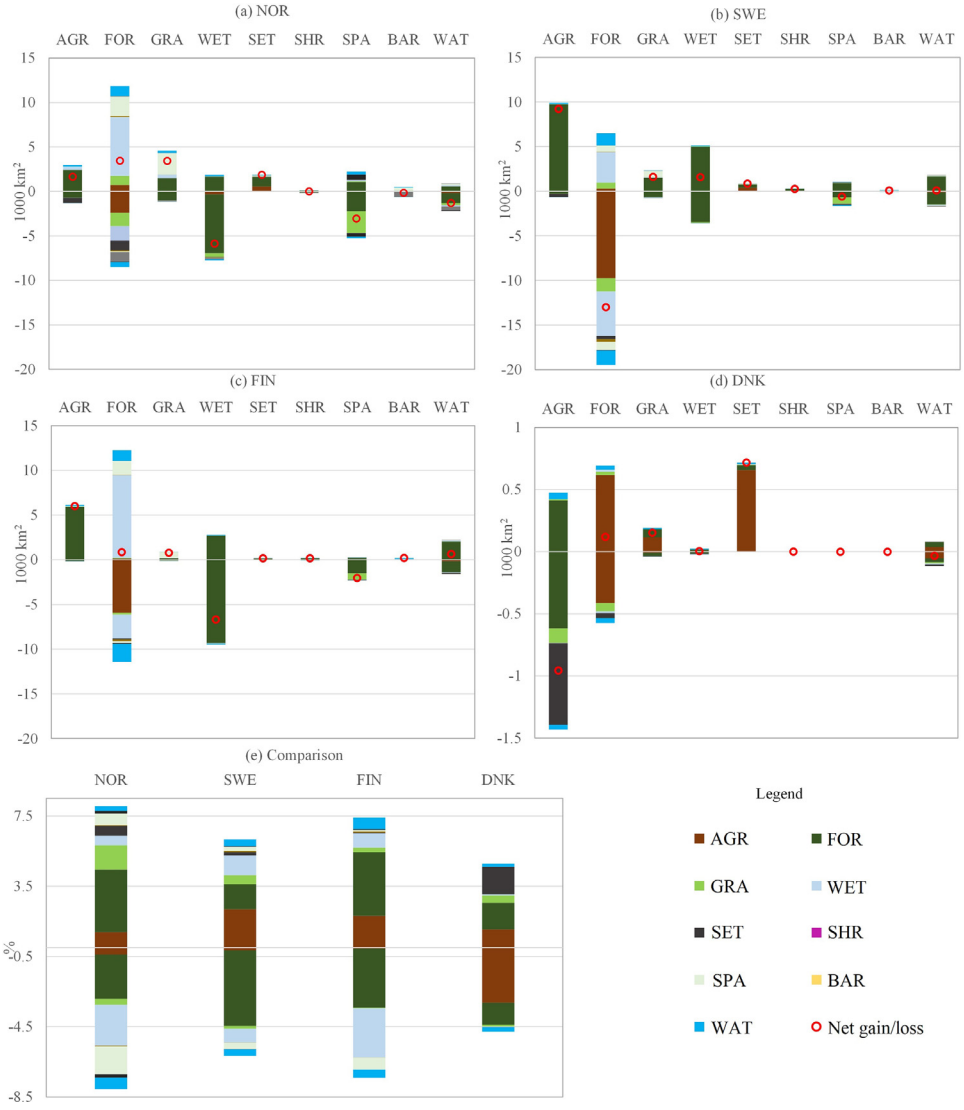

Fig. 2. Land cover transitions between 1992 and 2018 in (a) Norway (NOR), (b) Sweden (SWE), (c) Finland (FIN), (d) Denmark (DNK), and (e) comparison of land cover changes across countries. For (a)-(d), the different land cover types (IPCC classification system) are shown in the horizontal axis, and the vertical axis is the area changed of land cover. Positive values indicate a gross increase and negative values a gross decrease in the extent of the corresponding land covers (i.e., "converted to" if negative, and "converted from" if positive). Legend with different colors shows the type of land cover transitions. Red dots show the net gains or losses of each change. In (e), the vertical axis is the percentage change of each land cover relative to each country's total area, and the horizontal axis is for the four Nordic countries. AGR: agriculture, FOR: forest, GRA: grassland, WET: wetland, SET: settlement, SHR: shrubland, SPA: sparse vegetation, BAR: bare area.

Table 3
Comparison of changes in land cover in Norway (NOR), Sweden (SWE), Finland (FIN), Denmark (DNK) and in the entire region (Nordic) from 1992 to 2018 (Unit: 1,000 km^2). AGR: agriculture, FOR: forest, GRA: grassland, WET: wetland, SET: settlement, SHR: shrubland, SPA: sparse vegetation, BAR: bare area.

Region	AGR	FOR	GRA	WET	SET	SHR	SPA	BAR
NOR	+1.65	+3.44	+3.44	−5.87	+1.86	+0.01	−3.05	−0.17
SWE	+9.21	−13.01	+1.60	+1.56	+0.85	+0.25	−0.60	+0.07
FIN	+5.98	+0.84	+0.77	−6.70	+0.16	+0.16	−2.04	+0.20
DNK	−0.96	+0.12	+0.15	+0.004	+0.72	0.00	−0.001	−0.03
Nordic	+15.88	−8.61	+5.96	−11.00	+3.58	+0.41	−5.70	+0.10

Note: The values in the table show the absolute change of each land cover type from 1992 to 2018 in each country. Positive: net gains, negative: net loss, and 0.00: no change.

An overall comparison of the changes in land cover in the four countries is shown in Fig. 2e and Table 3. Land transitions typically involved from 4% to 9% of each country"s total area. The highest percentage of change in land cover is in Norway, followed by Finland, Sweden, and Denmark. The reduction of wetland in Norway and Finland made it the strongest net loss of a single class in the study region (11,003 km^2, −11%), followed by forest (8,607 km^2, −1%) and sparse vegetation (5,695 km^2, −7%). The area of forest in Sweden decreased, in contrast to the other three countries, which led to a decline in forest throughout the region. Other land covers such as agriculture, grassland, settlement, shrubland, and bare area, showed net increases. Agriculture area decreases in Denmark but increases in other three countries. Therefore, the agrculture area in Nordic region increases, as shown in Table 3.

3.3. Spatial distribution of land cover changes

Heat maps that identify major hotspots of changes in land cover are shown in Fig. 3. Agriculture decreased in Denmark and in coastal areas of Norway, and mainly increased in the southern part of Sweden

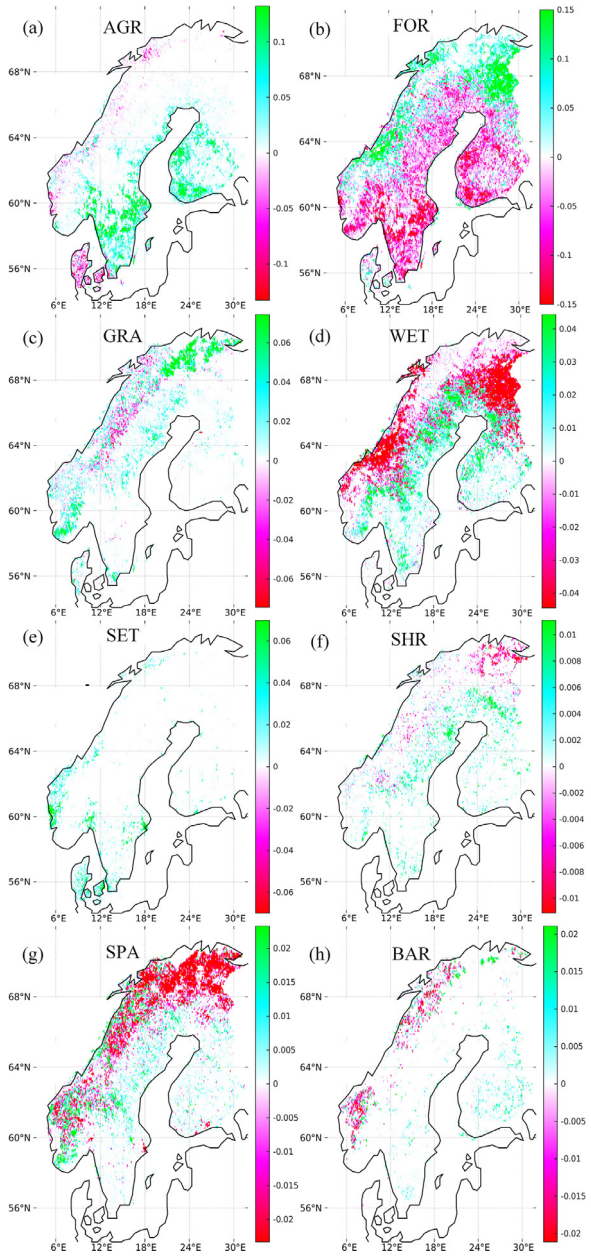

Fig. 3. Spatial distribution of land cover changes in Nordic countries. The value in the color bar shows the fraction of land cover change in each 9 km × 9 km grid cell from 1992 to 2018. A positive value indicates an increase and a negative value a decrease of the land cover. AGR: agriculture, FOR: forest, GRA: grassland, WET: wetland, SET: settlement, SHR: shrubland, SPA: sparse vegetation, BAR: bare area. Note that the scales of color bars are different in each subfigure. The aggregation from the original resolution of 300 m is for visualization purposes only.

and Finland. These dynamics can be associated with local and EU policies favoring local agriculture commodities, while cropland abandonment is often a result of socio-economic growth or, to smaller extent in EU, due to severe declines in soil fertility (Alcantara et al., 2013; Yin et al., 2020). Forest areas expanded especially in central Norway and the northern part of Nordic countries while they declined in Sweden, southern Norway and Finland. Major wetland declines occurred in Norway and northern Finland, typically on areas where forest expanded. Warming of climate in high latitude, availability of nutrient for plant growth and extensive water withdrawals are the main drivers of wetland drying (Werner et al., 2013; Green et al., 2017; Hu et al., 2021b). Wetland is an important ecosystem that regulates local climate and biodiversity, but it is highly sensitive to climate change and anthropogenic pressure (Ghajarnia et al., 2020). In the investigated CCI-LC dataset, wetland in Norway shows increasing declines mostly to forest and sparse vegetation. On the contrary, we find a small increase in wetland in Sweden (5%). This might reflect the outcome of major policy programs and efforts in Sweden to preserve wetlands, which even led to large-scale constructions of new wetlands with associated agro-environmental benefits to nutrient retention and biodiversity (Strand and Weisner, 2013). Sparse vegetation declined in the northern part of the analysis domain, mostly concomitant with expansion of grassland or forest, and this is related to the greening of the earth (Zhu et al., 2016). Settlement mainly increased in flat areas in the west and southern part of Nordic countries and around the main existing urban areas, and it might be linked to the growing population in the Nordic countries. Second homes in the Nordic region might also be a potential driver of settlement area increases (Müller, 2007; Larsson and Müller, 2019).

3.4. Forest harvest areas and their relationship with land cover transitions

The area of clear-cut forest harvest in Nordic countries and the potential overlap with the forest transitions to other land cover classes are shown in Table 4 and Fig. 4. The cumulative area of forest harvest between 2004 and 2018 is about 6,556 km^2 in Norway, 36,945 km^2 in Sweden, 29,158 km^2 in Finland, and 661 km^2 in Denmark. These numbers reflect the much larger forest management activities in Sweden and Finland than Norway, and the very limited operations in Denmark. There has been increasing trends in annual forest harvest areas in Sweden, Finland and Norway, especially in the latest period 2016–2018, when the three countries achieved their maximum clear-cut areas of 3,282 $km^2\ yr^{-1}$, 3,331 $km^2\ yr^{-1}$ and 647 $km^2\ yr^{-1}$, respectively (Fig. 4a). This trend might further increase according to future climate change mitigation scenarios that sustainable intensification of forestry to meet rising demands for renewable products and materials (Lauri et al., 2017; Hu et al., 2018; Verkerk et al., 2019). Denmark does not follow the same pattern and shows a negative trend in forest harvest area, largely due to limited forest resources in the country. Fig. 4b shows the spatial patterns of the cumulative forest harvested areas between 2004 and 2018. The most managed areas largely correspond to those with the largest presence of forest resources, and harvest intensity shows a clear pattern. Management activities are more intense in south Eastern Norway, and most parts of south and central Sweden and Finland, where they can be up to 20% of an aggregated grid cell. In the rest of Norway and in Northern Sweden and Finland forest harvested areas are much less abundant (less than 3%).

The locations of the forest to agriculture (FOR-to-AGR) or grassland (FOR-to-GRA) transitions between 2004 and 2018 from the CCI-LC dataset are shown in Fig. 4c and 4d, respectively. The transitions to shrubland and sparse vegetation are also considered, but not shown because of their smaller extent. A comparison between the areas where these transitions are detected and the areas of harvested forests from GFC dataset can inform about the extent to which forest cover disturbances caused by forest management are interpreted as forest transitions to other types of land cover by the CCI-LC dataset. Note that the comparison is done at the same resolution of the original CCI-LC dataset (300 m, to which the GFC data are aggregated), and the lower resolution of 9 km is only used in the figures to improve visualization. There is a non-negligible overlap between the CCI-LC-based transitions and the forest harvest areas. As shown in Table 4, between 10% (Norway) and 19% (Finland) of the areas identified as FOR-to-AGR transitions occurred in the same locations identified as clear-cut areas for the same time-period by the GFC database In absolute terms, FOR-to-AGR is the transition with the largest overlap, which is mainly found in Sweden (1,031 km^2), followed by Finland (617 km^2) and Norway (213 km^2). The overlap is largely distributed in central Sweden and southern Finland, where forest management activities are more intense (Fig. 4e). In

Table 4
Areas of forest harvest (1,000 km^2), annual average harvested area (1,000 km^2), area of forest to agriculture transition (1,000 km^2), and overlap between forest harvest areas and forest transitions from the CCI-LC dataset in absolute terms (1,000 km^2) and relative terms (%). FOR-to-AGR: forest to agriculture transition. FOR-to-GRA: forest to grassland transition. FOR-to-SHR: forest to shrubland transition. FOR-to-SPA: forest to sparse vegetation transition. NaN: not a number.

	Norway	Sweden	Finland	Denmark
Area of forest harvest (2004–2018)	6.6	36.9	29.2	0.7
Annual average area of forest harvest (2004–2018)	0.4	2.5	1.9	0.04
Area of FOR-to-AGR (2004–2018)	2.1	7.0	3.2	0.2
Overlap between harvested area and FOR-to-AGR	0.2	1.0	0.6	0.02
FOR-to-AGR in harvested area (%)[a]	10	15	19	11
Area of FOR-to-GRA (2004–2018)	0.7	1.1	0.2	0.05
Overlap between harvested area and FOR-to-GRA	0.01	0.5	0.1	$4.7*10^{-3}$
FOR-to-GRA in harvested area (%)[a]	2	51	49	11
Area of FOR-to-SHR (2004–2018)	0.08	0.2	0.2	0
Overlap between harvested area and FOR-to-SHR	0.01	0.1	0.07	0
FOR-to-SHR in harvested area (%)[a]	14	43	35	NaN
Area of FOR-to-SPA (2004–2018)	0.3	0.6	0.2	0
Overlap between harvested area and FOR-to-SPA	0.01	0.2	0.06	0
FOR-to-SPA in harvested area (%)[a]	5	40	30	NaN
Area of all CCI transitions	3.1	8.8	3.8	0.2
Overlap between all CCI transitions and harvested area	0.3	1.9	3.8	0.02
All CCI transitions in harvested area (%)[a]	8	21	22	11
Forest harvested area in all CCI transitions (%)[b]	4	5	3	3

[a] The percentage represents the overlap area divided by the forest transition area.
[b] The percentage represents the overlap area divided by the forest harvest area.

Table 5
Changes of soil erosion rate (unit: kg ha^{-1} yr^{-1}) on agriculture land in the Nordic countries. SER changes are weighted mean between 2012 and 2001 using pixel area as the weight, and values in the bracket is the standard error of the weighted mean. "Total" shows the total increased (positive values) or decreased (negative values) soil erosion in the period 2001–2012. SER: soil erosion rate.

	Norway	Sweden	Finland	Denmark
Average (standard error) SER in 2001	2,253 (20.7)	239 (0.97)	48.1 (0.19)	321 (0.56)
Average (standard error) SER in 2012	2,267 (20.7)	234 (0.96)	51.3 (0.18)	335 (0.59)
Average (standard error) change in SER	14.2 (0.23)	−4.95 (0.15)	3.17 (0.08)	14.2 (0.20)
Total (kt)	101	−91	46	245

relative terms, a much higher overlap is found between the FOR-to-GRA transitions and the clear-cut areas, where about 50% of the identified transitions in Sweden and Finland are actually located in forest harvest areas. However, this is inconsistent across Nordic countries (the overlap is only 2% in Norway), and it seems to be highly frequent (larger than 50%) in specific regions, such as central Sweden and scattered places in Finland. A similar result is obtained for the two other transitions (FOR-to-SHR and FOR-to-SPA), where their relevant overlap with clear-cut areas is higher in Sweden and Finland than Norway, and mostly located in central Sweden and some spots in Finland. A relevant share of forest transitions detected by the CCI-LC data are thus overlapping with forest harvest areas. When summed all together per country, between 8% and 22% of the detected transitions overlap with managed forest areas. As an alternative indicator to measure the integration of the two datasets, the fraction of the total forest harvest area that overlap with the forest transitions ranges from 3% (Finland) to 5% (Sweden). These numbers are lower because the percentage is calculated by dividing the overlap area by the total forest harvest area (which is larger than the forest transition area used for the ratios above).

In general, a key role is played by the specific management practices of the study region, which primarily involve small-scale harvest events that are difficult to be detected at the resolution of the CCI-LC data (300 m). For example, Sweden is the country with the largest overlap between forest transitions to other types of land cover and forest harvest. This can be explained by the average larger size of clear-cut areas in Sweden than other Nordic countries, which make these disturbances easier to detect by global land cover products. On the other hand, Denmark has the smallest average size of clear-cut and the lowest overlap between the two datasets. However, the largest share of temporary losses in forest cover due to forest management in Nordic countries are not detected by the CCI-LC dataset. A non-negligible fraction of them is instead classified as transitions to different types of land cover classes, mainly agriculture, but also grassland, shrubland or sparse vegetation.

3.5. Status and trends in soil erosion

Based on the integration of the ESA-CCI-LC (ESA, 2017) with a soil erosion dataset (Borrelli et al., 2017), soil erosion trends due to agriculture activities (e.g., areas which were classified as agriculture land both in 2001 and in 2012) in the Nordic countries are shown in Table 5 and Fig. 5. Areas experiencing soil erosion larger than 10 Mg ha^{-1} yr^{-1} are typically defined as affected by severe erosion rates, because they start to considerably lose their productivity (Panagos and Katsoyiannis, 2019; Prăvălie et al., 2021). However, soil conservation programs can also consider lower threshold values of approximately 5–12 Mg ha^{-1} yr^{-1}, and other studies recommend as a 'precautionary principle' to address soil erosion rates above 1 or 2 Mg ha^{-1} annually as they are already unsustainable in the long term (Prăvălie et al., 2021). In Nordic countries in 2012, the area of agricultural land with soil erosion rates higher than 5 Mg ha^{-1} yr^{-1} are 1,008 km^2 in Norway, 235 km^2 in Sweden, and 0 km^2 in both Finland and Denmark. If a lower threshold of soil erosion rate is considered (i.e., 1 Mg ha^{-1} yr^{-1}), the agricultural land requiring interventions are 2,541 km^2 in Norway, 1,471 km^2 in Sweden, 0.2 km^2 in Finland, and 2,674 km^2 in Denmark.

Compared to global trends (Borrelli et al., 2017; Hu et al., 2021b), changes in SERs between 2001 and 2012 in Nordic countries are relatively small (Fig. 5a). The highest increases in rates of soil erosion in agricultural land from 2001 to 2012 occurred in Norway and Denmark

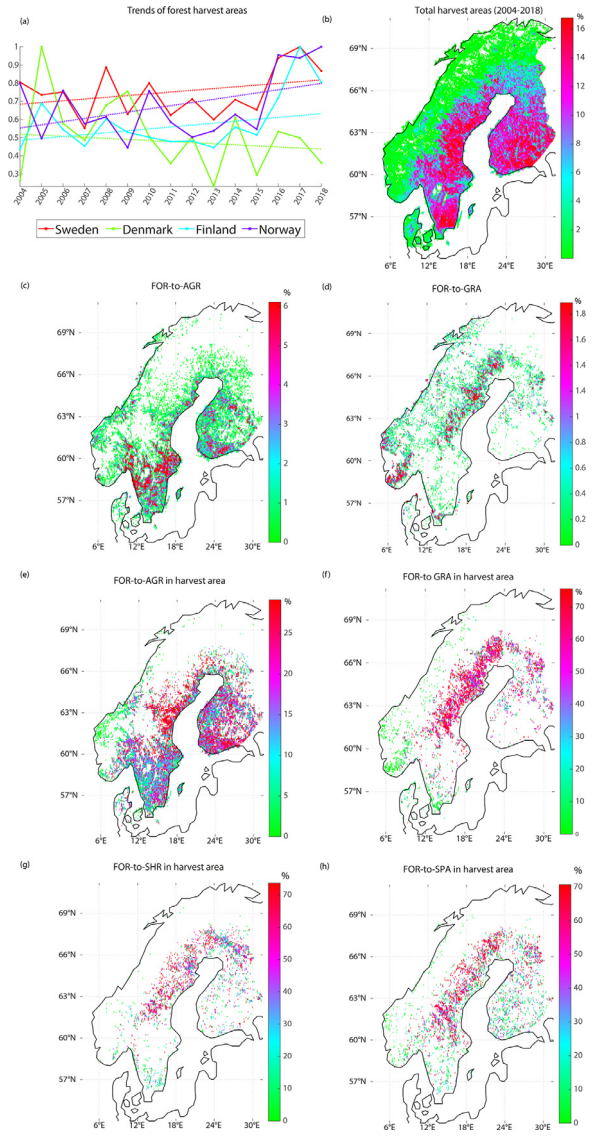

Fig. 4. Clear-cut areas in Nordic countries and potential overlaps with forest transitions identified by the CCI-LC dataset. Forest harvest trends (a), spatial distributions of cumulative harvested forest (2004–2018) (b), forest to agriculture (FOR-to-AGR) transition (c), forest to grassland (FOR-to-GRA) transitions (d), overlap between harvest forest areas and FOR-to-AGR (e), overlap between harvest forest and FOR-to-GRA transitions (f), overlap between harvest forest area and forest to shrubland (FOR-to-SHR) transitions (g) and overlap between harvest forest areas and forest to sparse vegetation (FOR-to-SPA) transitions (h). In (a), the solid lines are the areas of annual forest harvest normalized to their maximum values (Sweden: 3,282, Denmark: 86, Finland: 3,331, Norway: 647, unit: km^2), and the dotted lines are the linear fit of the temporal trend. In (b)–(h), maps are aggregated to 9 km resolution to improve visualization. Note that the scales of color bars are different in each subfigure.

(about 14.2 ± 0.2 kg ha^{-1} yr^{-1}), followed by Finland (3.2 ± 0.1 kg ha^{-1} yr^{-1}), and the rates are much lower than the global average changes in SERs in agricultural land reported by Borrelli et al. (2017) and Hu et al. (2021b). The change of SER in Sweden is negative, meaning that the soil erosion is mitigated between 2001 and 2012. The average low soil erosion rates in Nordic countries are probably due to more sustainable agriculture practices than other places in the world, although the SERs increases in some locations, such as southern Sweden and Finland (Fig. 5b). Norway and Denmark have areas which are classified as potentially unsustainable (SER higher than 1 Mg ha^{-1} yr^{-1}) in the long term (Fig. 5c), but only Norway has regions that are suffering high SER (higher than 5 Mg ha^{-1} yr^{-1}), especially on the coastal area (Fig. 5d), which would require urgent mitigation measures.

4. Discussions

Our analysis is based on two recently released high spatial resolution land cover products, the ESA-CCI-LC, and C3S-CDS-LC products. Detailed quantitative analyses were performed to depict the major trends in land cover dynamics and spatial distribution patterns in four Nordic countries. There have been multiple validation efforts of this dataset (Hua et al., 2018; Li et al., 2018; Liu et al., 2018a). An average global accuracy of 71% has been estimated with variations among land cover types and regions (ESA, 2017). In Finland, the overall accuracy of the ESA-CCI-LC dataset is 64%, but accuracy typically increase when the 37 subclasses are aggregated to broader classes as done here. For example, when it is used as a forest product the accuracy in Finland is 88%, with misclassifications mainly occurring in the far north. Another study estimated an overall accuracy of the ESA-CCI-LC product of 64% in the Arctic Circle (Liang et al., 2019).

Limitations of the ESA-CCI-LC and C3S-CDS-LC products are mainly from possible misclassifications. Wetland, shrubland and sparse vegetation have a higher uncertainty than classes such as cropland and forest, which are typically registered with higher accuracy (ESA, 2017). It follows that transitions involving land cover classes that have larger uncertainty are less robust than transitions between two land cover classes with higher certainty, such as forest to agriculture (and vice versa) transitions. Besides, the accuracies of the individual land cover vary in these two land cover datasets. For instance, the accuracy of urban class in the C3S-CDS-LC dataset has been improved relative to that in the ESA-CCI-LC dataset. These aspects should be considered when interpreting the results of our study.

The land cover change is detected by the ESA-CCI-LC product when it is confirmed over two consecutive years (ESA, 2017), and this aspect influences the changes between two adjacent years and for the first three years (1992–1994) of the time series. The spatial resolution of the land cover dataset is 300 m, meaning that only changes in land cover of certain size can be detected. This may also influence the accuracy at which CCI-LC data can capture changes happening along the coastlines.

Our study shows that, maybe due to the small scale at which forest management activities are undertaken in Nordic countries, the majority of forest cover clearance is not detected by the CCI-LC dataset. A certain fraction that varies by country and land cover types is identified as forest transitions to agriculture or grassland (and to a smaller extent to shrubland and sparse vegetation). These aspects should be considered when further improving the accuracy of the land cover products. The maps used to identify forest harvest areas are also subject to uncertainties, which have been discussed in detail in the original study (Ceccherini et al., 2020) and following commentaries (Palahí et al., 2021; Wernick et al., 2021) and rebuttal (Ceccherini et al., 2021). The capacity of the GFC maps to detect forest loss has been validated (Ceccherini et al., 2020), and uncertainties are found to be lower in some years compared to others and for large patches (forest patch size greater than 0.27 ha) than fragmented areas. The classification accuracy is particularly high (more than 82% correct detection) for patches larger than 4.5 ha. Arguments on the limitations of these forest harvest maps include aspects such as reported changes may reflect analytical artefacts with inconsistencies in the forest change time series, uncertain factors in the algorithm used to identify forest harvest area, misattribution of natural disturbances as harvests, and a lack of causality with the suggested bioeconomy policy frameworks (Palahí et al., 2021; Wernick et al., 2021). Especially, the abrupt changes typically observed in the period 2016-2018 are essentially an artefact stemming from incorrect use of the GFC data time series, as similar trends are observed in other regions of the globe (Palahí et al., 2021). Further, the GFC dataset has a high resolution of about 30 m and is able to record clear-cuts of a given size, but small-scale removals and thinning operations cannot be

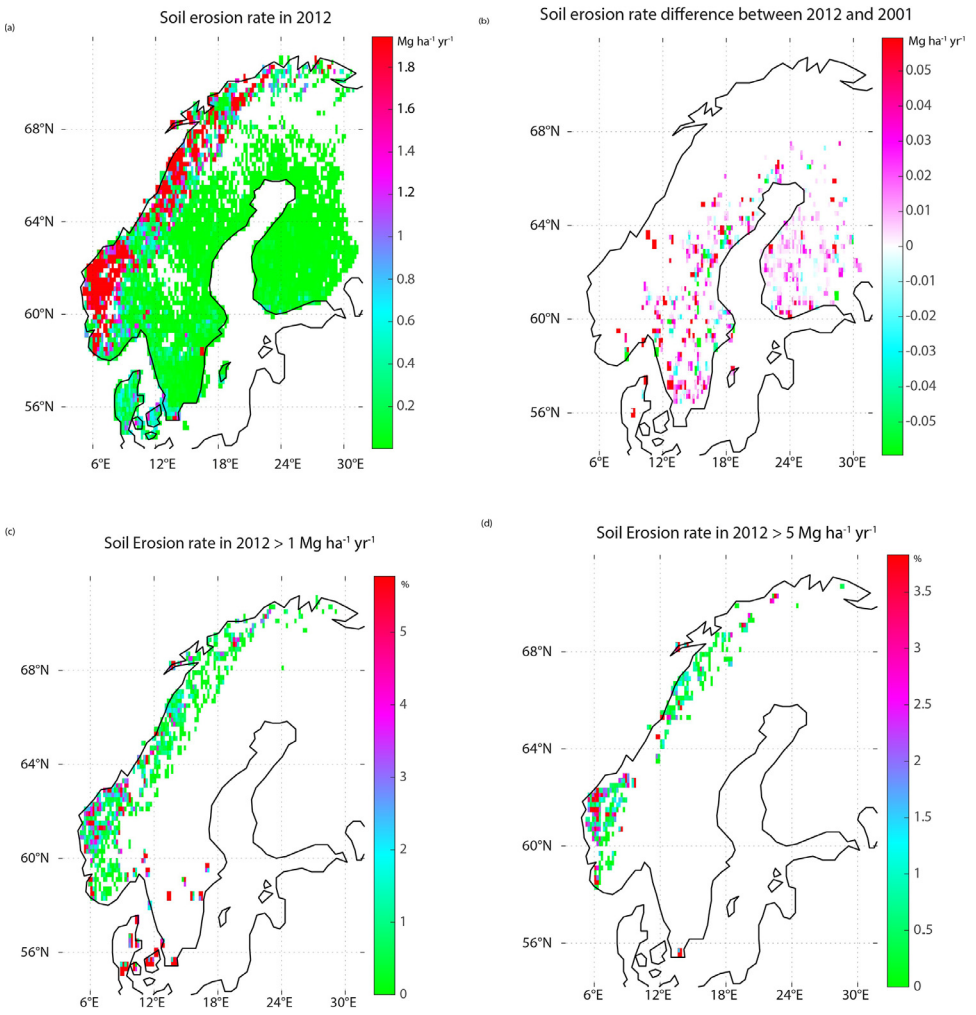

Fig. 5. Spatial distribution of soil erosion rate and increased total soil erosion in agricultural land. Soil erosion rate in 2012 (a), soil erosion rate change between 2012 and 2001 (b), areas with soil erosion rate higher than 1 Mg ha^{-1} yr^{-1} (c), areas with soil erosion rate higher than 5 Mg ha^{-1} yr^{-1} (d). Maps in (c) and (d) are aggregated to 24 km spatial resolution to improve visualization, and the values show the percentages of area above the given thresholds in the aggregated grids. Agriculture land refers to the grid cells classified as agriculture land both in 2001 and 2012.

seen by the satellite when the change in crown cover is not large enough to be detected.

Forest management represents a challenge when compiling large-scale global datasets of land cover time series. Given the long-term climatic and environmental implications of forest management (Naudts et al., 2016; Huang et al., 2020), it is highly beneficial to establish a clearer representation in global land cover datasets of forested areas and transitional, age-dependent, forest dynamics, so to facilitate the modelling of their effects by climate and ecosystem models (Cherubini et al., 2018b; Lindeskog et al., 2021). Our analysis shows the potential to integrate the CCI-LC products and the GFC-based forest harvest maps to improve the representation of global land cover dynamics, but technical challenges for a successful integration still remain. Future studies should explore the extent to which these datasets overlap, and the type of forest transitions involved, especially in areas with forest management activities that are distinctly different than those used in Nordic counties. Ideally, the representation of forest management areas in global land cover datasets would require the definition of a new land cover class for a unique identification of this type of temporal transition (from a technical point of view, harvested areas are to be classified as forest remaining forest). More collective international efforts are needed to obtain high quality data at different temporal and spatial levels representative of forest management and dynamics (Palahí et al., 2021).

The analysis of SER also has limitations. Two major potential issues are the resolution of the SER maps and land cover dataset used by Borrelli et al. (2017). Compared to the resolution of the CCI-LC dataset, the spatial resolution of SER maps is low, which means that some changes in SER cannot be detected with a coarser resolution. Further, the SER maps used a different land cover dataset than in our study, and the mismatch of the land cover classes can be a source of uncertainty. Future high-resolution maps of SER with consistent land cover dataset can thus help to more accurately quantify SER changes related to land use and land cover changes.

5. Conclusions

Understanding the spatio-temporal dynamics of land use change is critical to address global environmental challenges such as food security, climate change, and biodiversity loss. We combined and reclassified the ESA-CCI-LC and C3S-CDS-LC products to measure changes in land cover from 1992 to 2018 in Norway, Denmark, Sweden, and Finland, and analyze the trends and spatial distributions of the transitions. We found extensive land cover dynamics in these countries, with different spatial patterns, that are the results of direct human interferences and/or climate change. For example, settlements expanded the most in relative terms, and wetland shrinkage is a major transition in the Northern part of the study area. The trend is concerning given the key role that wetlands play in regulating the local climate and supporting a variety of ecosystem services, including biodiversity, and deserves closer (ground-level) monitoring and the implementation of mitigation measures. Overall, our results offer insights on the main characteristics of these datasets on changes in land cover and are instrumental to future studies applying these data in land surface models, climate models, landscape ecology, or similar applications.

Investigating the relationships between the maps of forest harvest areas and forest transitions to different types of land cover shows that the majority of forest cover clearance goes undetected in the CCI-LC dataset, likely because they occur at a much finer scale than the resolution of the CCI-LC dataset. However, a non-negligible share of the forest transitions to agriculture or grassland happened in the same locations identified as managed forest areas. This shows a potential for a representation of forest management in global land cover products, which facilitate the possibility of including their effects by climate and ecosystem models that rely on these datasets. On average, soil erosion rates in agriculture land in the four Nordic countries are generally lower compared to other places in the world, but there are areas experiencing high soil erosion rates, especially in western Norway, which require mitigation measures to prevent irreversible declines in soil fertility and ecosystem services. Possible extensions of the current analysis include integrating land cover products with other datasets such as climate variables and/or environmental attributes, or comparing the overlap of CCI-derived land cover transitions with harvested areas in other places with remarkably different practices in forest management than Nordic countries.

About three-quarters of the Earth's land surface has already been affected by human activities, and land cover are key to regulate climate services, provide habitat to species and support food supply. In particular, the role of soil fertility in agricultural land and sustainable forest management underpins the realization of a variety of sustainable development goals. To better understand land cover changes and the main drivers (human pressures, climate change, natural disturbances, and forest management, etc.), there is an increasing need for international coordination to produce maps that integrate different sources of information across various spatial and temporal levels, so to overcome inconsistencies and limitations of individual datasets. This knowledge is crucial to develop science-based policies that can prevent adverse land use changes and preserve ecosystem services given the rising pressures on land resources for natural conservation, food, and renewable energy supply and materials under the threats posed by ongoing climate change.

Declarations of Competing Interest

The authors declare that there is no known competing financial interests or personal relationships that could have appeared to influence the work reported in this paper.

Acknowledgements

This research was funded by the Norwegian Research Council (Grant No. 286773), the National Natural Science Foundation of China (Grant No. 41861134038) through the CHINOR bilateral research project MitiStress, China Scholarship Council (Grant No. 201906410051) and the Fundamental Research Funds for National Universities, China University of Geosciences (Wuhan) (Grant No. 2201710266). Hu acknowledges the help from Dr. Ceccherini for the forest harvested maps.

References

Alcantara, C., Kuemmerle, T., Baumann, M., Bragina, E.V., Griffiths, P., Hostert, P., Knorn, J., Müller, D., Prishchepov, A.V., Schierhorn, F., 2013. Mapping the extent of abandoned farmland in Central and Eastern Europe using MODIS time series satellite data. Environ. Res. Lett. 8, 035035.

Arsanjani, J.J., Helbich, M., de Noronha Vaz, E., 2013. Spatiotemporal simulation of urban growth patterns using agent-based modeling: The case of Tehran. Cities 32, 33–42.

Auffret, A.G., Kimberley, A., Plue, J., Waldén, E., 2018. Super-regional land-use change and effects on the grassland specialist flora. Nat. Commun. 9, 1–7.

Aune, S., Bryn, A., Hovstad, K.A., 2018. Loss of semi-natural grassland in a boreal landscape: impacts of agricultural intensification and abandonment. J. Land Use Sci. 13, 375–390.

Bartholome, E., Belward, A.S., 2005. GLC2000: A new approach to global land cover mapping from Earth observation data. Int. J. Remote Sens. 26, 1959–1977.

Borrelli, P., Robinson, D.A., Fleischer, L.R., Lugato, E., Ballabio, C., Alewell, C., Meusburger, K., Modugno, S., Schutt, B., Ferro, V., Bagarello, V., Van Oost, K., Montanarella, L., Panagos, P., 2017. An assessment of the global impact of 21st century land use change on soil erosion. Nat. Commun. 8, 1–13.

Borrelli, P., Robinson, D.A., Panagos, P., Lugato, E., Yang, J.E., Alewell, C., Wuepper, D., Montanarella, L., Ballabio, C., 2020. Land use and climate change impacts on global soil erosion by water (2015-2070). PNAS 117, 21994–22001.

Bryn, A., Potthoff, K., 2018. Elevational treeline and forest line dynamics in Norwegian mountain areas–A review. Landsc. Ecol. 33, 1225–1245.

C3S, 2019. Land cover classification gridded maps from 1992 to present derived from satellite observations.

Ceccherini, G., Duveiller, G., Grassi, G., Lemoine, G., Avitabile, V., Pilli, R., Cescatti, A., 2020. Abrupt increase in harvested forest area over Europe after 2015. Nature 583, 72–77.

Ceccherini, G., Duveiller, G., Grassi, G., Lemoine, G., Avitabile, V., Pilli, R., Cescatti, A., 2021. Reply to Wernick, I.K. et al. ; Palahí, M. et al.. Nature 592, E18–E23.

Chen, J., Chen, J., Liao, A., Cao, X., Chen, L., Chen, X., He, C., Han, G., Peng, S., Lu, M., 2015. Global land cover mapping at 30 m resolution: A POK-based operational approach. ISPRS J. Photogramm. Remote Sens. 103, 7–27.

Cherubini, F., Huang, B., Hu, X.P., Tolle, M.H., Stromman, A.H., 2018a. Quantifying the climate response to extreme land cover changes in Europe with a regional model. Environ. Res. Lett. 13, 074002.

Cherubini, F., Santaniello, F., Hu, X.P., Sonesson, J., Stromman, A.H., Weslien, J., Djupstrom, L.B., Ranius, T., 2018b. Climate impacts of retention forestry in a Swedish boreal pine forest. J. Land Use Sci. 13, 301–318.

Cherubini, F., Vezhapparambu, S., Bogren, W., Astrup, R., Stromman, A.H., 2017. Spatial, seasonal, and topographical patterns of surface albedo in Norwegian forests and cropland. Int. J. Remote Sens. 38, 4565–4586.

Crooks, K.R., Burdett, C.L., Theobald, D.M., King, S.R., Di Marco, M., Rondinini, C., Boitani, L., 2017. Quantification of habitat fragmentation reveals extinction risk in terrestrial mammals. PNAS 114, 7635–7640.

De Vente, J., Poesen, J., 2005. Predicting soil erosion and sediment yield at the basin scale: Scale issues and semi-quantitative models. Earth-Sci. Rev. 71, 95–125.

Duveiller, G., Caporaso, L., Abad-Vinas, R., Perugini, L., Grassi, G., Arneth, A., Cescatti, A., 2020. Local biophysical effects of land use and land cover change: Towards an assessment tool for policy makers. Land Use Policy 91, 104382.

EFFIS, 2019. Statistics Portal. https://gwis.jrc.ec.europa.eu/apps/gwis_current_situation/index.html [Accessed 16 Febrary 640 2021].

ESA, 2017. Land Cover CCI: Product User Guide Version 2.0. https://maps.elie.ucl.ac.be/CCI/viewer/download/ESACCI-LC-Ph2-PUGv2_2.0.pdf [Accessed 643 May, 27th 2020].

FAO, 2020. FAOSTAT Datebase. http://www.fao.org/faostat/en [Accessed Dec, 645 12th 2020].

Fourcade, Y., Åström, S., Öckinger, E., 2019. Climate and land-cover change alter bumblebee species richness and community composition in subalpine areas. Biodivers. Conserv. 28, 639–653.

Friedl, M.A., McIver, D.K., Hodges, J.C., Zhang, X.Y., Muchoney, D., Strahler, A.H., Woodcock, C.E., Gopal, S., Schneider, A., Cooper, A., 2002. Global land cover mapping from MODIS: Algorithms and early results. Remote Sens. Environ. 83, 287–302.

Gava, O., Bartolini, F., Venturi, F., Brunori, G., Pardossi, A., 2020. Improving policy evidence base for agricultural sustainability and food security: A content analysis of life cycle assessment research. Sustainability 12, 1033.

Ghajarnia, N., Destouni, G., Thorslund, J., Kalantari, Z., Åhlén, I., Anaya-Acevedo, J.A., Blanco-Libreros, J.F., Borja, S., Chalov, S., Chalova, A., 2020. Data for wetlandscapes and their changes around the world. Earth Syst. Sci. Data 12, 1083–1100.

Gomes, E., Abrantes, P., Banos, A., Rocha, J., Buxton, M., 2019. Farming under urban pressure: Farmers' land use and land cover change intentions. Appl. Geogr. 102, 58–70.

Gorelick, N., Hancher, M., Dixon, M., Ilyushchenko, S., Thau, D., Moore, R., 2017. Google Earth Engine: Planetary-scale geospatial analysis for everyone. Remote Sens. Environ. 202, 18–27.

Green, A.J., Alcorlo, P., Peeters, E.T., Morris, E.P., Espinar, J.L., Bravo-Utrera, M.A., Bustamante, J., Díaz-Delgado, R., Koelmans, A.A., Mateo, R., 2017. Creating a safe operating space for wetlands in a changing climate. Front. Ecol. Environ. 15, 99–107.

Grekousis, G., Mountrakis, G., Kavouras, M., 2015. An overview of 21 global and 43 regional land-cover mapping products. Int. J. Remote Sens. 36, 5309–5335.

Hansen, M.C., Potapov, P.V., Moore, R., Hancher, M., Turubanova, S.A., Tyukavina, A., Thau, D., Stehman, S., Goetz, S.J., Loveland, T.R., 2013. High-resolution global maps of 21st-century forest cover change. Science 342, 850–853.

Henriksen, S., Hilmo, O., 2015. Norsk rødliste for arter 2015. Artsdatabanken, Norge 6.

Hu, X., Huang, B., Verones, F., Cavalett, O., Cherubini, F., 2021a. Overview of recent land-cover changes in biodiversity hotspots. Front. Ecol. Environ. 19, 91–97.

Hu, X., Næss, J.S., Iordan, C.M., Huang, B., Zhao, W., Cherubini, F., 2021b. Recent global land cover dynamics and implications for soil erosion and carbon losses from deforestation. Anthropocene 34, 100291.

Hu, X.P., Huang, B., Cherubini, F., 2019. Impacts of idealized land cover changes on climate extremes in Europe. Ecol. Indic. 104, 626–635.

Hu, X.P., Iordan, C.M., Cherubini, F., 2018. Estimating future wood outtakes in the Norwegian forestry sector under the shared socioeconomic pathways. Global Environ. Change 50, 15–24.

Hua, T., Zhao, W.W., Liu, Y.X., Wang, S., Yang, S.Q., 2018. Spatial consistency assessments for global land-cover datasets: A comparison among GLC2000, CCI LC, MCD12, GLOBCOVER and GLCNMO. Remote Sens. 10, 1846.

Huang, B., Hu, X.P., Fuglstad, G.A., Zhou, X., Zhao, W.W., Cherubini, F., 2020. Predominant regional biophysical cooling from recent land cover changes in Europe. Nat. Commun. 11, 1–13.

Hurtt, G.C., Chini, L., Sahajpal, R., Frolking, S., Bodirsky, B.L., Calvin, K., Doelman, J.C., Fisk, J., Fujimori, S., Klein Goldewijk, K., 2020. Harmonization of global land use change and management for the period 850–2100 (LUH2) for CMIP6. Geosci. Model Dev. 13, 5425–5464.

Iordan, C.M., Hu, X., Arvesen, A., Kauppi, P., Cherubini, F., 2018a. Contribution of forest wood products to negative emissions: historical comparative analysis from 1960 to 2015 in Norway, Sweden and Finland. Carbon Balance Manag. 13, 12.
Iordan, C.M., Verones, F., Cherubini, F., 2018b. Integrating impacts on climate change and biodiversity from forest harvest in Norway. Ecol. Indic. 89, 411–421.
IPCC, 2019. Summary for Policymakers. In: Shukla, J.S.P.R., Calvo Buendia, E., Masson-Delmotte, V., Pörtner, H.- O., Roberts, D.C., Zhai, P., Slade, R., Connors, S., van Diemen, R., Ferrat, M., Haughey, E., Luz, S., Neogi, S., Pathak, M., Petzold, J., Portugal Pereira, J., Vyas, P., Huntley, E., Kissick, K., Belkacemi, M., Malley, J. (Eds.), Climate Change and Land: An IPCC special report on climate change, desertification, land degradation, sustainable land management, food security, and greenhouse gas fluxes in terrestrial ecosystems. IPCC, pp. 1–36 In press.
Karvonen, V., Ribard, C., Sädekoski, N., Tyystjärvi, V., Muukkonen, P., 2018. Comparing ESA land cover data with higher resolution national datasets. In: Tyystjärvi, V., Muukkonen, P. (Eds.), Creating, managing, and analysing geospatial data and databases in geographical themes. University of Helsinki, Helsinki, pp. 26–45.
Kellomäki, S., Strandman, H., Heinonen, T., Asikainen, A., Venäläinen, A., Peltola, H., 2018. Temporal and spatial change in diameter growth of boreal Scots pine, Norway spruce, and birch under recent-generation (CMIP5) global climate model projections for the 21st century. Forests 9, 118.
Larsson, L., Müller, D.K., 2019. Coping with second home tourism: Responses and strategies of private and public service providers in western Sweden. Curr. Issues Tour. 22, 1958–1974.
Lauri, P., Forsell, N., Korosuo, A., Havlík, P., Obersteiner, M., Nordin, A., 2017. Impact of the 2 C target on global woody biomass use. Forest Policy Econ. 83, 121–130.
Leclère, D., Obersteiner, M., Barrett, M., Butchart, S.H., Chaudhary, A., De Palma, A., DeClerck, F.A., Di Marco, M., Doelman, J.C., Dürauer, M., 2020. Bending the curve of terrestrial biodiversity needs an integrated strategy. Nature 585, 551–556.
Leirpoll, M.E., Næss, J.S., Cavalett, O., Dorber, M., Hu, X., Cherubini, F., 2021. Optimal combination of bioenergy and solar photovoltaic for renewable energy production on abandoned cropland. Renew. Energ. 168, 45–56.
Li, W., MacBean, N., Ciais, P., Defourny, P., Lamarche, C., Bontemps, S., Houghton, R.A., Peng, S.S., 2018. Gross and net land cover changes in the main plant functional types derived from the annual ESA CCI land cover maps (1992-2015). Earth Syst. Sci. Data 10, 219–234.
Liang, L., Liu, Q., Liu, G., Li, H., Huang, C., 2019. Accuracy evaluation and consistency analysis of four global land cover products in the Arctic region. Remote Sens. 11, 1396.
Lindeskog, M., Lagergren, F., Smith, B., Rammig, A., 2021. Accounting for forest management in the estimation of forest carbon balance using the dynamic vegetation model LPJ-GUESS (v4. 0, r9333): Implementation and evaluation of simulations for. Europe. Geosci. Model Dev. Discuss. 1–42.
Liu, X.X., Yu, L., Li, W., Peng, D.L., Zhong, L.H., Li, L., Xin, Q.C., Lu, H., Yu, C.Q., Gong, P., 2018a. Comparison of country-level cropland areas between ESA-CCI land cover maps and FAOSTAT data. Int. J. Remote Sens. 39, 6631–6645.
Liu, X.X., Yu, L., Si, Y.L., Zhang, C., Lu, H., Yu, C.Q., Gong, P., 2018b. Identifying patterns and hotspots of global land cover transitions using the ESA CCI Land Cover dataset. Remote Sens. Lett. 9, 972–981.
Lohila, A., Minkkinen, K., Laine, J., Savolainen, I., Tuovinen, J.P., Korhonen, L., Laurila, T., Tietäväinen, H., Laaksonen, A., 2010. Forestation of boreal peatlands: Impacts of changing albedo and greenhouse gas fluxes on radiative forcing. J. Geophy. Res. 115, G04011.
Loveland, T.R., Belward, A., 1997. The international geosphere biosphere programme data and information system global land cover data set (DISCover). Acta Astronaut. 41, 681–689.
Lukes, P., Stenberg, P., Mottus, M., Manninen, T., Rautiainen, M., 2016. Multidecadal analysis of forest growth and albedo in boreal Finland. Int. J. Appl. Earth Obs. Geoinf. 52, 296–305.
Mienna, I.M., Speed, J.D.M., Klanderud, K., Austrheim, G., Næsset, E., Bollandsås, O.M., 2020. The relative role of climate and herbivory in driving treeline dynamics along a latitudinal gradient. J. Veg. Sci. 31, 392–402.
Milberg, P., Bergman, K.-O., Jonason, D., Karlsson, J., Westerberg, L., 2019. Land-use history influence the vegetation in coniferous production forests in southern Sweden. For. Ecol. Manage. 440, 23–30.
Mousivand, A., Arsanjani, J.J., 2019. Insights on the historical and emerging global land cover changes: The case of ESA-CCI-LC datasets. Appl. Geogr. 106, 82–92.
Müller, D.K., 2007. Second homes in the Nordic countries: Between common heritage and exclusive commodity. Scand. J. Hosp. Tourism 7, 193–201.
Myers-Smith, I.H., Kerby, J.T., Phoenix, G.K., Bjerke, J.W., Epstein, H.E., Assmann, J.J., John, C., Andreu-Hayles, L., Angers-Blondin, S., Beck, P.S., 2020. Complexity revealed in the greening of the Arctic. Nat. Clim. Change 10, 106–117.
Næss, J.S., Cavalett, O., Cherubini, F., 2021. The land–energy–water nexus of global bioenergy potentials from abandoned cropland. Nat. Sustain. 4, 525–536.
Naudts, K., Chen, Y., McGrath, M.J., Ryder, J., Valade, A., Otto, J., Luyssaert, S., 2016. Europe's forest management did not mitigate climate warming. Science 351, 597–600.
Nunes, J.R., Loures, L., Lopez-Piñeiro, A., Loures, A., Vaz, E., 2016. Using GIS towards the characterization and soil mapping of the caia irrigation perimeter. Sustainability 8, 368.
Osei-Owusu, A.K., Kastner, T., de Ruiter, H., Thomsen, M., Caro, D., 2019. The global cropland footprint of Denmark's food supply 2000–2013. Global Environ. Chang. 58, 101978.
Palahí, M., Valbuena, R., Senf, C., Acil, N., Pugh, T.A., Sadler, J., Seidl, R., Potapov, P., Gardiner, B., Hetemäki, L., 2021. Concerns about reported harvests in European forests. Nature 592, E15–E17.
Panagos, P., Katsoyiannis, A., 2019. Soil erosion modelling: The new challenges as the result of policy developments in Europe. Elsevier.
Pei, J., Niu, Z., Wang, L., Song, X.-P., Huang, N., Geng, J., Wu, Y.-B., Jiang, H.-H., 2018. Spatial-temporal dynamics of carbon emissions and carbon sinks in economically developed areas of China: A case study of Guangdong Province. Sci. Rep. 8, 1–15.
Plieninger, T., Draux, H., Fagerholm, N., Bieling, C., Bürgi, M., Kizos, T., Kuemmerle, T., Primdahl, J., Verburg, P.H., 2016. The driving forces of landscape change in Europe: A systematic review of the evidence. Land Use Policy 57, 204–214.
Plummer, S., Lecomte, P., Doherty, M., 2017. The ESA climate change initiative (CCI): A European contribution to the generation of the global climate observing system. Remote Sens. Environ. 203, 2–8.
Prăvălie, R., Patriche, C., Borrelli, P., Panagos, P., Roşca, B., Dumitraşcu, M., Nita, I.-A., Săvulescu, I., Birsan, M.-V., Bandoc, G., 2021. Arable lands under the pressure of multiple land degradation processes. A global perspective. Environ. Res. 194, 110697.
Räsänen, A., Nygren, A., Monge, A.M., Käkönen, M., Kanninen, M., Juhola, S., 2018. From divide to nexus: Interconnected land use and water governance changes shaping risks related to water. Appl. Geogr. 90, 106–114.
Ren, W., Banger, K., Tao, B., Yang, J., Huang, Y., Tian, H., 2020. Global pattern and change of cropland soil organic carbon during 1901-2010: Roles of climate, atmospheric chemistry, land use and management. Geogr. Sustain. 1, 59–69.
Roe, S., Streck, C., Obersteiner, M., Frank, S., Griscom, B., Drouet, L., Fricko, O., Gusti, M., Harris, N., Hasegawa, T., 2019. Contribution of the land sector to a 1.5°C world. Nat. Clim. Change 9, 817–828.
Saco, P.M., Moreno-de las Heras, M., Keesstra, S., Baartman, J., Yetemen, O., Rodríguez, J.F., 2018. Vegetation and soil degradation in drylands: Non linear feedbacks and early warning signals. Curr. Opin. Env. Sci. Health 5, 67–72.
Schelhaas, M.-J., Fridman, J., Hengeveld, G.M., Henttonen, H.M., Lehtonen, A., Kies, U., Krajnc, N., Lerink, B., Ní Dhubháin, Á., Polley, H., 2018. Actual European forest management by region, tree species and owner based on 714,000 re-measured trees in national forest inventories. PLoS One 13, e0207151.
Smith, P., Calvin, K., Nkem, J., Campbell, D., Cherubini, F., Grassi, G., Korotkov, V., Le Hoang, A., Lwasa, S., McElwee, P., 2020. Which practices co-deliver food security, climate change mitigation and adaptation, and combat land degradation and desertification? Glob. Chang. Biol. 26, 1532–1575.
Song, X.-P., Hansen, M.C., Stehman, S.V., Potapov, P.V., Tyukavina, A., Vermote, E.F., Townshend, J.R., 2018. Global land change from 1982 to 2016. Nature 560, 639–643.
Strand, G.-H., 2013. The Norwegian area frame survey of land cover and outfield land resources. Nor. Geografisk Tidsskr.-Norw. J. Geogr. 67, 24–35.
Strand, J.A., Weisner, S.E., 2013. Effects of wetland construction on nitrogen transport and species richness in the agricultural landscape—Experiences from Sweden. Ecol. Eng. 56, 14–25.
Strassburg, B.B., Iribarrem, A., Beyer, H.L., Cordeiro, C.L., Crouzeilles, R., Jakovac, C.C., Junqueira, A.B., Lacerda, E., Latawiec, A.E., Balmford, A., 2020. Global priority areas for ecosystem restoration. Nature 586, 724–729.
Szogs, S., Arneth, A., Anthoni, P., Doelman, J.C., Humpenöder, F., Popp, A., Pugh, T.A., Stehfest, E., 2017. Impact of LULCC on the emission of BVOCs during the 21st century. Atmos. Environ. 165, 73–87.
Taubert, F., Fischer, R., Groeneveld, J., Lehmann, S., Müller, M.S., Rödig, E., Wiegand, T., Huth, A., 2018. Global patterns of tropical forest fragmentation. Nature 554, 519–522.
Ulén, B., Bechmann, M., Øygarden, L., Kyllmar, K., 2012. Soil erosion in Nordic countries—Future challenges and research needs. Acta Agr. Scand. B–S. P. Sci. 62, 176–184.
van Vliet, J., 2019. Direct and indirect loss of natural area from urban expansion. Nat. Sustain. 2, 755–763.
Vauhkonen, J., Packalen, T., 2018. Uncertainties related to climate change and forest management with implications on climate regulation in Finland. Ecosyst. Serv. 33, 213–224.
Venter, O., Sanderson, E.W., Magrach, A., Allan, J.R., Beher, J., Jones, K.R., Possingham, H.P., Laurance, W.F., Wood, P., Fekete, B.M., 2016. Sixteen years of change in the global terrestrial human footprint and implications for biodiversity conservation. Nat. Commun. 7, 1–11.
Verkerk, P.J., Fitzgerald, J.B., Datta, P., Dees, M., Hengeveld, G.M., Lindner, M., Zudin, S., 2019. Spatial distribution of the potential forest biomass availability in. Europe. For. Ecosyst. 6, 1–11.
Vogdrup-Schmidt, M., Olsen, S.B., Dubgaard, A., Kristensen, I.T., Jørgensen, L.B., Normander, B., Ege, C., Dalgaard, T., 2019. Using spatial multi-criteria decision analysis to develop new and sustainable directions for the future use of agricultural land in Denmark. Ecol. Indic. 103, 34–42.
Wehn, S., Olsson, G., Hanssen, S., 2012. Forest line changes after 1960 in a Norwegian mountain region–implications for the future. Nor. Geografisk Tidsskr.-Norw. J. Geogr. 66, 2–10.
Werner, B.A., Johnson, W.C., Guntenspergen, G.R., 2013. Evidence for 20th century climate warming and wetland drying in the North American Prairie Pothole Region. Ecol. Evol. 3, 3471–3482.
Wernick, I.K., Ciais, P., Fridman, J., Högberg, P., Korhonen, K.T., Nordin, A., Kauppi, P.E., 2021. Quantifying forest change in the European Union. Nature 592, E13–E14.
Yin, H., Brandão Jr„ A., Buchner, J., Helmers, D., Iuliano, B.G., Kimambo, N.E., Lewińska, K.E., Razenkova, E., Rizayeva, A., Rogova, N., 2020. Monitoring cropland abandonment with Landsat time series. Remote Sens. Environ. 246, 111873.
Zhu, Z.C., Piao, S.L., Myneni, R.B., Huang, M.T., Zeng, Z.Z., Canadell, J.G., Ciais, P., Sitch, S., Friedlingstein, P., Arneth, A., Cao, C.X., Cheng, L., Kato, E., Koven, C., Li, Y., Lian, X., Liu, Y.W., Liu, R.G., Mao, J.F., Pan, Y.Z., Peng, S.S., Penuelas, J., Poulter, B., Pugh, T.A.M., Stocker, B.D., Viovy, N., Wang, X.H., Wang, Y.P., Xiao, Z.Q., Yang, H., Zaehle, S., Zeng, N., 2016. Greening of the Earth and its drivers. Nat. Clim. Change 6, 791–795 -+.